



## Influence of Electron Donor/Acceptor Concentrations on Hydrous Ferric Oxide (HFO) Bioreduction

James K. Fredrickson, Sreenivas Kota, Ravi K. Kukkadapu, Chongxuan Liu & John M. Zachara  
Pacific Northwest National Laboratory, Richland, WA 99352, USA (\*author for correspondence: e-mail: jim.fredrickson@pnl.gov)

Accepted 28 March 2003

**Key words:** bioreduction, hydrous ferric oxide, mineralization, *Shewanella putrefaciens*

### Abstract

Dissimilatory metal-reducing bacteria (DMRB) facilitate the reduction of Fe and Mn oxides in anoxic soils and sediments and play an important role in the cycling of these metals and other elements such as carbon in aqueous environments. Previous studies investigating the reduction of Fe(III) oxides by DMRB focused on reactions under constant initial electron donor (lactate) and electron acceptor (Fe oxide) concentrations. Because the concentrations of these reactants can vary greatly in the environment and would be expected to influence the rate and extent of oxide reduction, the influence of variable electron acceptor and donor concentrations on hydrous ferric oxide (HFO) bioreduction was investigated. Batch experiments were conducted in pH 7  $\text{HCO}_3^-$  buffered media using *Shewanella putrefaciens* strain CN32. In general, the rate of Fe(III) reduction decreased with increasing HFO:lactate ratios, resulting in a relatively greater proportion of crystalline Fe(III) oxides of relatively low availability for DMRB. HFO was transformed to a variety of crystalline minerals including goethite, lepidocrocite, and siderite but was almost completely dissolved at high lactate to HFO ratios. These results indicate that electron donor and acceptor concentrations can greatly impact the bioreduction of HFO and the suite of Fe minerals formed as a result of reduction. The respiration driven rate of Fe(II) formation from HFO is believed to be a primary factor governing the array of ferrous and ferric iron phases formed during reduction.

### Introduction

Microbial metal reduction is an important process in the oxidation of organic matter in a wide variety of sedimentary environments (Lovley 1993; Nealson & Saffarini 1994) and, as a result of their metabolism, dissimilatory metal-reducing bacteria (DMRB) have a profound influence on the aqueous geochemistry and mineralogy of sedimentary environments (Baedecker et al. 1992; Heron & Christensen 1995). In addition, microbial metal reduction can influence the fate and transport of organic (Lovley et al. 1989b) and inorganic contaminants (Lovley 1995; Lovley & Lloyd 2000).

Fe(III) and Mn(IV) oxides are insoluble at the pH of most natural waters and therefore differ from other common electron acceptors for microbial metabolism such as  $\text{O}_2$ ,  $\text{NO}_3^-$ ,  $\text{SO}_4^{2-}$  and  $\text{CO}_2$ . As a result, the

relationships between microorganisms and electron acceptor and electron donor utilization are complex and poorly understood (Zachara et al. 2002). In natural environments, poorly crystalline hydrous ferric oxide (HFO) or two-line ferrihydrite has been suggested as a principal form of Fe(III) oxide reduced by some DMRB (Lovley & Phillips 1986, 1987). Crystalline Fe(III) oxides such as goethite and hematite are also reducible to varying degrees by some DMRB (Arnold et al. 1988; Roden & Zachara 1996) but the factors governing the availability of Fe(III) oxides for microbial reduction are poorly understood. Surface area (Roden & Zachara 1996), crystalline disorder and microheterogeneities (Zachara et al. 1998) are but a few of the factors that appear to influence the rate and extent of microbial reduction of Fe oxides. Sorption of Fe(II) to oxide and cell surfaces (Urrutia et al. 1998) and the formation of soluble Fe(II)-organic complexes

(Urrutia et al. 1999) or removal of Fe(II) by advective transport (Roden & Urrutia 1999; Roden et al. 2000) are additional factors that can influence the microbial reduction of Fe(III) oxides.

The majority of previous studies investigating biogeochemical controls on microbial Fe(III) oxide reduction have been conducted in medium or buffer with high concentrations of electron donor and acceptor (Roden & Zachara 1996; Fredrickson et al. 1998; Urrutia et al. 1998; Zachara et al. 1998; Roden & Urrutia 1999; Roden et al. 2000; Kukkadapu et al. 2001). In natural environments, however, the concentrations of electron acceptor/donor may vary greatly over small spatial scales. It is unclear how these variations may influence the rate and extent of Fe(III) oxide reduction and the types of biominerals that are formed as a result.

Laboratory studies investigating various aspects of HFO bioreduction have, in general, been performed using high concentrations of HFO (>40 mM) and excess donor concentrations (Lovley & Phillips 1988; Lovley et al. 1989a; Roden & Lovley 1993; Roden & Zachara 1996; Fredrickson et al. 1998; Zachara et al. 1998). The rates and extents of HFO reduction in these studies were influenced by the type of electron donor, solution composition, and inoculum size. A series of experiments with *Shewanella putrefaciens* strain CN32 revealed that the reduction and biomineralization of HFO was significantly influenced by the solution composition (Fredrickson et al. 1998). In experiments with 45 mM HFO and 27 mM lactate, greater than 84% of the HFO was reduced in pH 7 bicarbonate buffered solutions. The resulting solids were dominated by siderite ( $\text{FeCO}_3$ ) and magnetite ( $\text{Fe}_3\text{O}_4$ ). In contrast, 32–52% of the HFO was reduced in PIPES buffered solutions in the absence of  $\text{PO}_4^{3-}$  and AQDS (anthraquinone-2, 6-disulfonate) and magnetite was the dominant phase formed. When  $\text{PO}_4^{3-}$  and AQDS were present in PIPES, the extent of reduction was significantly greater (>70%), and the resulting solid phase was predominantly a green rust  $[\text{Fe}_{(6-x)}^{\text{II}}\text{Fe}_x^{\text{III}}(\text{OH})_{12}]^{x+}[(\text{A}^{2-})_x/2 \cdot y\text{H}_2\text{O}]^{x-}$ . The types of biominerals formed can have important implications to geomicrobial processes in sediments and soil. For example, if magnetite is the dominant end product of HFO reduction, approximately 2/3 of the Fe(III) may be rendered unavailable for subsequent microbial reduction except under select chemical conditions (Kostka & Nealson 1995; Dong et al. 2000). The types of biominerals formed as a result of HFO reduction can also have important impacts on the fate and chemical behavior of trace metals (Fredrickson

et al. 2001). An important issue yet to be explored is whether comparable minerals and rates and extents of HFO reduction would result under varying Fe(III) (HFO, as the electron acceptor) and electron donor (lactate) concentrations that may better reflect environmental variations.

In this research, we report investigations into the influence of electron donor (HFO)/acceptor (lactate) concentrations on bacterial reduction of HFO by the DMRB *S. putrefaciens* CN32. Specific objectives of this work were to identify the secondary minerals formed and compare rates and extent of reduction under varying electron donor:acceptor ratios to gain predictive and mechanistic insights.

## Experimental procedures

### *Bacteria and media*

*S. putrefaciens* strain CN32 was provided courtesy of Dr. David Boone (Portland State University, DOE Subsurface Microbial Culture Collection). Details regarding the isolation and culturing of this organism have been described previously (Fredrickson et al. 1998; Zachara et al. 1998). CN32 has been used extensively in our laboratory to study reduction of Fe(III) in single phase oxides and in sediments. Cells were harvested from mid to late log phase in aerobic tryptic soy broth (TSB) cultures by centrifugation, washed with buffer to remove residual TSB, resuspended in 30 mM, pH 7 bicarbonate buffer, and purged with  $\text{N}_2:\text{CO}_2$ . Cells were added to the media to obtain a final concentration of  $2 \times 10^8 \text{ mL}^{-1}$ .

The composition of basal medium used for HFO reduction was (mM):  $\text{NH}_4\text{Cl}$  (28.0),  $\text{Na}_2\text{HPO}_4$  (0.44),  $\text{KCl}$  (1.20),  $\text{CaCl}_2 \cdot 2\text{H}_2\text{O}$  (0.61), and  $\text{NaHCO}_3$  (30.0). The medium was supplemented with 10 mL each of vitamin and trace mineral solutions described previously (Lovley & Phillips 1988). L-lactic acid (ICN biochemicals) served as electron donor. The medium was dispensed into 60 mL serum bottles, purged with  $\text{O}_2$ -free  $\text{N}_2:\text{CO}_2$  (80:20), stoppered with butyl rubber closures, and crimp sealed.

Poorly crystalline hydrous ferric oxide was prepared by neutralization of a  $\text{FeCl}_3 \cdot 6\text{H}_2\text{O}$  solution with  $\text{NaOH}$  to pH 7 followed by repeated washing with deionized water to remove chloride and sodium. This procedure can yield akaganeite as a product if the pH is not rapidly neutralized to approximately 7. Care was taken to avoid akaganeite precipitation and the

synthetic product obtained yielded X-ray diffraction patterns and Mössbauer spectra consistent with 2-line ferrihydrite. In previous investigations using identical synthesis procedures for 2-line ferrihydrite a surface area of  $240 \text{ m}^2 \text{ g}^{-1}$  was measured (Roden & Zachara 1996). We term this material hydrous ferric oxide (HFO) for simplicity. The HFO product was maintained as an aqueous suspension for  $\sim 72$  h prior to addition to the media to obtain the desired final concentrations. Bottles were incubated at  $25^\circ\text{C}$  and agitated at 100 rpm. Each treatment consisted of two live (w/CN32 cells) and one control (no cells) in respective serum bottles.

An Fe(II) standard solution used for abiotic experiments was prepared by dissolving  $\text{FeCl}_2$  in 20 mM PIPES buffer. The solution pH was measured and made anaerobic by purging with  $\text{O}_2$ -free  $\text{N}_2$ . All titrations were conducted in an anaerobic glove bag and the stock solution filtered ( $0.2 \mu\text{m}$ ) prior to addition.

#### *Fe(II)-facilitated HFO transformation*

To investigate the possible abiotic transformation of HFO by Fe(II), 50 mM HFO in pH 7 bicarbonate buffer was equilibrated with 20 mM PIPES buffered solutions with varying Fe(II) concentrations under anaerobic conditions at  $25^\circ\text{C}$  for 4 weeks. At the end of the equilibration period the pH of the suspensions was measured and the solids were analyzed by XRD to identify the dominant mineral phases.

#### *Analyses*

During the course of the experiments, treatments were monitored for increase in Fe(II) production and depletion of lactate. Serum bottles were repeatedly sampled under anaerobic and aseptic conditions during the course of an experiment. Sampled suspensions (0.5 mL) were filtered ( $0.2 \mu\text{m}$  polycarbonate) directly into 0.5 mL of 0.5 N Ultrex HCl. This filtrate was considered as the soluble fraction. HCl-extractable Fe was obtained by placing 0.5 mL of suspension directly into 0.5 mL of 1 N Ultrex HCl, mixing, and equilibrating for 24 h before analyzing for Fe(II) and Fe(total). Samples for lactate analysis were collected by placing 0.5 mL of suspension directly into 0.5 mL of 0.1 N NaOH.

Fe(II) in acidified filtrates ( $0.2 \mu\text{m}$ ) or extracts was determined using the ferrozine assay (Lovley & Phillips 1986). For Fe(total), samples were first reacted in 0.25 N hydroxylamine hydrochloride to reduce Fe(III) to Fe(II) prior to analysis by the ferrozine assay.

Lactate concentrations were determined using lactate reagent (Sigma Diagnostics, St. Louis, MO).

#### *X-ray diffraction*

Mineral residues from the reduction experiments were dried in an anaerobic glovebag and smeared on a glass slide for X-ray diffraction (XRD) analysis. The slides were maintained under anoxic conditions until analyzed. The apparatus consisted of two Phillips Wide-Range Vertical goniometers with incident-beam 2-theta compensating slits, soller slits, fixed 2 mm receiving slits, diffracted beam graphite monochromators, and scintillation counter detectors. The X-ray source was a Phillips XRG3100 X-ray generator operating a fixed-anode, long-fine-focus Cu tube at 45 Kv, 40 mA (1800 W). Instrument control was by means of Databox NIMBIM modules (Materials Data, Inc., Livermore, CA).

#### *Mössbauer spectroscopy*

Random orientation absorbers were prepared by mixing 17–28 mg of anaerobically dried sample with petroleum jelly in a 0.5-in. or 3/8-in. thick and 0.5-in. I.D. Cu holder sealed at one end with clear scotch tape. The sample space was filled with petroleum jelly and the ends sealed with the tape. The samples were prepared and stored under an anaerobic atmosphere. Spectra were collected at room temperature (RT) using  $\sim 50$  mCi (1.85 MBq)  $^{57}\text{Co}/\text{Rh}$  single-line thin sources. 77 K measurements were carried out using a top-loading Janis exchange-gas cryostat with entire source-drive assembly at RT. The Mössbauer bench (MB-500; WissEL, Germany) was equipped with a dual Mössbauer drive system to gather data simultaneously for two experiments. The velocity transducer (MVT-1000; WissEL) operated in the constant-acceleration mode ( $23 \text{ Hz} \pm 10 \text{ mm/s}$ ). Data were acquired on 1024 channels and then folded to 512 channels to give a flat background and a zero-velocity position corresponding to the center shift (CS or  $\delta$ ) of a metallic-Fe foil at room temperature. Calibration spectra were obtained with a  $20\text{-}\mu\text{m}$  thick  $\alpha\text{-Fe}$  foil (Amersham, England) placed in exactly the same position as the samples to minimize error due to changes in geometry. The transmitted radiation was recorded with Ar-Kr proportional counters. The unfolded spectra obtained were folded and evaluated with Recoil (University of Ottawa, Canada) program using Voigt-based hyperfine parameter distribution method (Rancourt & Ping 1991).

## Results

### Variable HFO and constant lactate

Microbial reduction of HFO was monitored for 370 h during which time the concentrations of 0.5 N HCl-extractable Fe(II), aqueous Fe(II) and lactate were measured. Extraction with 0.5 N HCl is effective in solubilizing most biogenic Fe<sup>2+</sup> solid phases including magnetite (Fredrickson et al. 1998) and it is used here as a measure of the total extent of reduction. The rate of HFO reduction was initially slow but was followed by a rapid increase before cessation of reduction at ~300 h for most of the treatments (Figures 1a, b). The initial lag was most apparent at the highest HFO concentrations and, for the 100 mM HFO treatment, there was little Fe(III) reduction prior to 100 h. These results are in contrast to previous investigations into the bioreduction of Fe(III) by CN32 where no lag phase was observed under similar conditions but with 45 mM HFO and 18–20 mM lactate (Fredrickson et al. 1998).

Soluble Fe(II) increased with time (Figure 1a) as did the HCl-extractable Fe(II) (Figure 1b) reflecting the progression of HFO bioreduction by CN32. The extent of reduction after incubation for 370 h, however, varied with the initial HFO concentration as did the concentration of aqueous Fe(II) (Table 1). Aqueous Fe(II) concentrations were significantly lower than the total (HCl extracted) Fe(II) except at the lowest HFO concentrations. At 5 and 10 mM HFO the solid was almost completely dissolved and >90% of the Fe(II) was in the soluble form after 370 h (Table 1). Fe(II) is strongly sorbed by HFO at circumneutral pH and can form mixed valence solids such as magnetite and green rust or can be complexed by a variety of ligands that can precipitate as Fe(II) minerals. Phosphate is one such ligand that can complex Fe(II) and precipitate as vivianite [Fe<sub>3</sub>(PO<sub>4</sub>)<sub>2</sub>·8H<sub>2</sub>O]. The phosphate (PO<sub>4</sub><sup>3-</sup>) concentration used in the experiments reported herein was relatively low (0.44 mM) and would have had only a minor effect on Fe(II) solubility. Although HFO was reduced nearly to completion at the lowest HFO concentrations, at 25 mM and higher the extent of reduction as a percentage of the total Fe(III) decreased as the initial HFO concentration increased (Table 1).

Crystalline ferric and ferrous minerals were observed in the various treatments at the termination of the experiment. At the lowest HFO concentration the Fe(III) was nearly quantitatively reduced. Upon visual

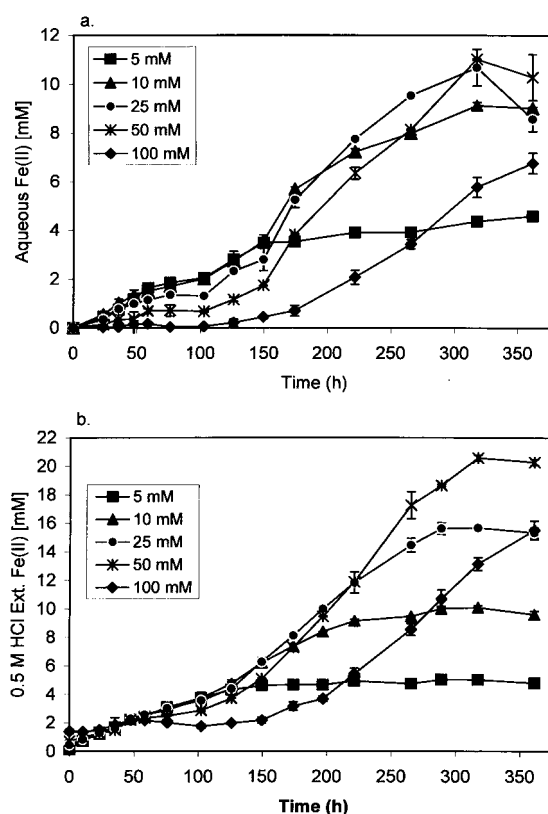


Figure 1. HFO bioreduction under varying HFO concentrations (5–100 mM) and constant lactate (30 mM): (a) Fe(II)<sub>aq</sub> concentrations; (b) 0.5 M HCl-extractable Fe(II). Error bars represent standard deviation for two replicates.

Table 1. Mineral solids (XRD, geochemical analysis), % reduction, % transformed to crystalline minerals for variable HFO and constant lactate (30 mM) experiment

HFO (mM)	% Reduction <sup>b</sup>	PH <sup>a</sup> (final)	Fe(II) <sub>aq</sub> <sup>a</sup> mM	Predominant mineral phases (XRD)
5	91.8	6.56	4.59	Nd <sup>b</sup>
10	91.3	6.89	9.13	Nd <sup>b</sup>
25	61.4	6.66	10.69	Siderite
50	40.56	7.65	11.01	Siderite, Goethite
100	15.52 <sup>a</sup>	6.70	6.76	Goethite

<sup>a</sup> After 350 h. Sampling terminated.

<sup>b</sup> Nd – not determined.

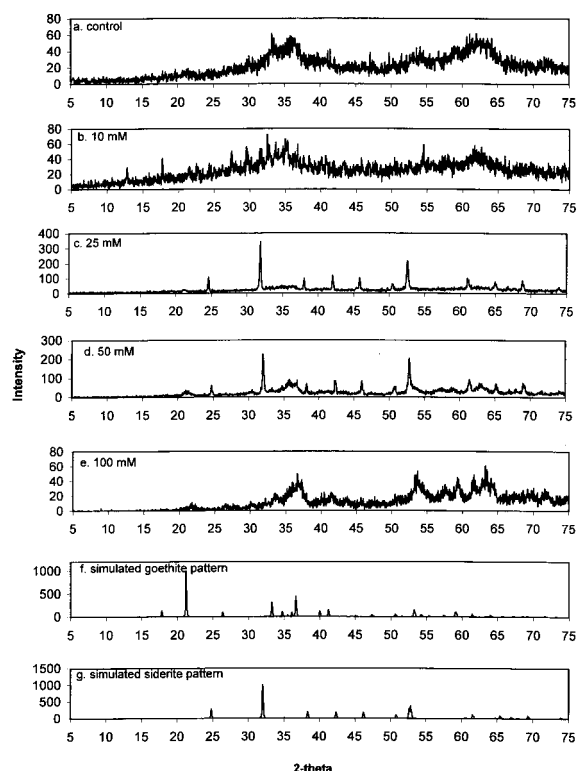


Figure 2. X-ray diffractograms of microbially reduced HFO under varying HFO concentrations: (a) Control (50 mM HFO, unreduced), (b) 25 mM, (c) 50 mM and (d) 100 mM. Note: No XRD analysis was performed on 5 and 10 mM HFO samples because of inadequate sample size.

inspection, there was a small amount of solid material remaining after reduction of the 5 mM HFO treatment but the quantity was insufficient to analyze by XRD or Mössbauer spectroscopy. The calculated saturation indices (S.I.) suggested that the solution was saturated with respect to siderite ( $\text{FeCO}_3$ ). In the 25 and 50 mM HFO treatments the presence of siderite was confirmed by XRD (Figures 2c, d). At 50 mM HFO the crystalline Fe(III) oxide goethite ( $\alpha\text{-FeOOH}$ ) was present in addition to siderite and dominated the solid phase at 100 mM although the diffractogram for this sample exhibited a relatively low signal-to-noise ratio (Figure 2e). The transformation of HFO to crystalline Fe(III) oxides by DMRB at very low electron acceptor to donor ratios is consistent with previous findings (Zachara et al. 2002).

#### Variable lactate and constant HFO

In the variable lactate experiments, reduction of the 50 mM HFO commenced immediately after inoculation

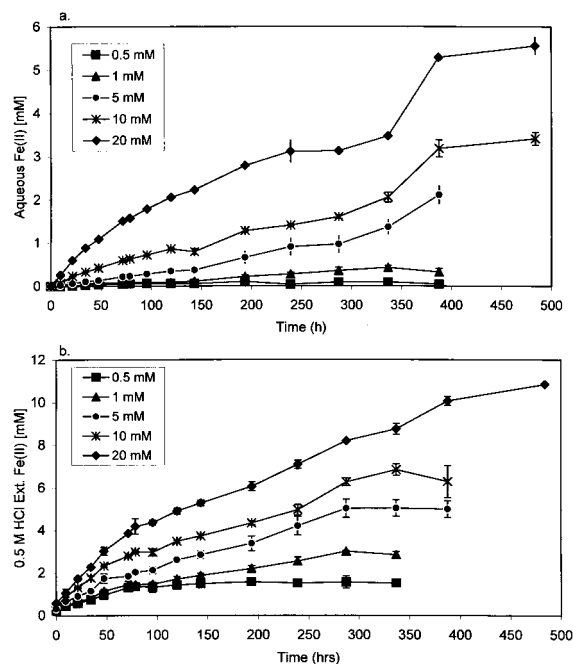


Figure 3. HFO bioreduction under varying lactate concentrations (0.5–20 mM) and constant HFO (50 mM): (a)  $\text{Fe(II)}_{\text{aq}}$  concentrations; (b) 0.5 M HCl-extractable Fe(II). Error bars represent standard deviation for two replicates.

without an apparent lag (Figure 3). This is in contrast to HFO reduction in the variable HFO concentration experiments, but is in agreement with our previous study on HFO bioreduction by CN32 where little or no lag in HFO reduction was observed (Fredrickson et al. 1998). The effect of varying lactate concentration on HFO reduction was clearly evident from the initial rates and final extent of HFO reduction (Figure 3; Table 2). Initial Fe(III) reduction rates increased from 14.3 to 50  $\mu\text{mol h}^{-1}$  and the extent of HFO reduction increased from 2.8 to 19.7% as the initial lactate concentration increased from 0.5 to 20 mM.

As anticipated, increases in Fe(III) reduction were accompanied by decreases in lactate concentration (Figure 4). Lactate was completely consumed at the 0.5 and 1 mM concentrations while significant amounts remained at higher initial concentrations. Assuming a theoretical ratio of 1:4 for lactate oxidized (to  $\text{CO}_2$  and acetate) to Fe(III) reduced (Fredrickson et al. 1998) there was near stoichiometric consumption of lactate coupled to Fe(III) reduced at 0.5 and 1 mM lactate treatments but at higher lactate concentrations the efficiency of lactate oxidation coupled to Fe(III) reduction decreased significantly (Table 2). At higher lactate concentrations of 5, 10, and 20 mM the

Table 2. Mineral solids (XRD, Mössbauer and geochemical analysis), first order rates, % reduction, % transformed to crystalline minerals for constant HFO (50 mM) and variable lactate experiment

Lactate (mM)	Initial rates ( $\mu\text{moles/h}$ ) <sup>a</sup>	% Reduction <sup>b</sup>	% Crystalline Fraction <sup>b</sup>	pH <sup>b</sup>	Fe(II) <sub>aq</sub> <sup>b</sup> mM	% Theoretical Mass. (lactate conversion) <sup>b</sup>	Mineral phases	
							XRD	Mössbauer
0.5	14.3	2.8	29.7	6.93	0.09	95	Goethite, Lepidocrocite	Goethite, Lepidocrocite, Siderite
1	17.7	5.3	36.73	6.99	0.43	92.9	Goethite, Lepidocrocite, Siderite	Nd <sup>c</sup>
5	27	9.2	29.52	6.90	2.11	42.3	Goethite, Siderite	Goethite, Siderite
10	39	12.7	28.38	6.98	3.41	31.9	Goethite, Siderite	Nd <sup>c</sup>
20	50	19.7	10.35	7.03	5.56	51.8	Goethite, Siderite	Goethite, Siderite

<sup>a</sup>Initial rates were assumed to be linear during the first 50 hr.

<sup>b</sup>After 350 hr.

<sup>c</sup>Nd- not determined.

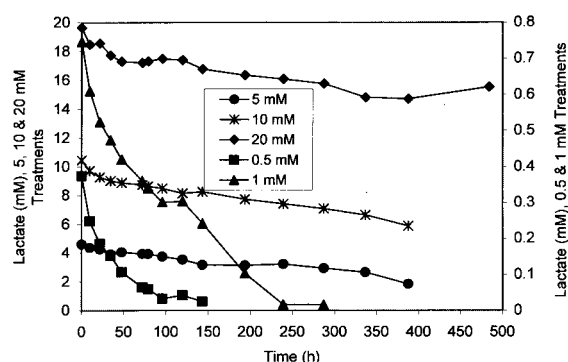


Figure 4. Variation in lactate measurements with time in the variable lactate experiment.

efficiencies of lactate oxidation were comparable to previous reports of 51% of the theoretical maximum for 45 mM HFO and 27 mM lactate in experiments with CN32 (Fredrickson et al. 1998).

Soluble Fe(II) concentrations were again consistently lower than concentrations of Fe(II) extracted by 0.5 N HCl indicating that sorption or precipitation dominated the partitioning of biogenic Fe(II) (Figure 3). The fraction of total Fe(II) (0.5 M HCl-extractable) in the aqueous phase increased with increasing lactate concentrations (Table 2). At 0.5 and 1 mM lactate, the fraction of the total Fe(II) in the aqueous phase was <15% compared to >40% at 5, 10 and 20 mM lactate. Greater reduction rates coupled with decreasing HFO sorption sites, a consequence of HFO mass loss were one reason for the dependence of Fe(II)<sub>aq</sub> on lactate concentration. Another was the potential

aqueous complexation of Fe(II) by residual lactate or acetate. Unfortunately the complexation constants of Fe(II) with these ligands are small and not sufficiently quantified to allow defensible speciation calculations.

The incomplete utilization of lactate in spite of sufficient residual Fe(III), especially at 5, 10 and 20 mM HFO, may be attributed to several factors. A solid residue was observed after the 0.5 N HCl extraction of the bio-reduced HFO at 5, 10, and 20 mM lactate (Figure 4). Previous studies demonstrated that HFO, siderite and fine-grained biogenic magnetite are completely dissolved in 0.5 M HCl (Fredrickson et al. 1998). Crystalline Fe(III) oxides such as goethite and hematite are poorly soluble in 0.5 M HCl (Sidhu et al. 1981). Therefore, it was hypothesized that HFO transformation to crystalline Fe oxides may have decreased the pool of easily reducible Fe(III) that, in turn, limited lactate consumption. In order to further evaluate this hypothesis, changes in 0.5 M HCl extractable total iron [Fe(II + III)<sub>T</sub>] were also measured. These analyses indicated that there was a decrease in Fe<sub>T</sub> extracted with 0.5 N HCl over time at all lactate concentrations (Figure 5). The acid extractable Fe<sub>T</sub> decreased with decreasing initial lactate concentration (Figure 5). This suggests that the incomplete oxidation of lactate, in spite of significant concentrations of residual Fe(III), may have been due, in part, to the transformation of HFO into crystalline Fe(III) oxides that were less reducible than HFO. There were other factors involved, however, because the percent lactate utilization did not correlate well with acid extractable Fe<sub>T</sub>.

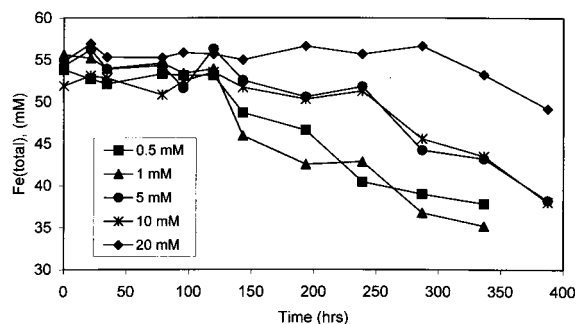


Figure 5. Fe(total) measurements on varying lactate (0.5–20 mM) and constant HFO treatments. Decrease in the amount of Fe(total) indicates conversion to crystalline products not extracted by 0.5 M HCl.

X-ray diffraction analysis of residual solids following bioreduction (Figure 6) revealed a diverse range of Fe mineral phases (Table 2). Interpretation of XRD spectra suggested that goethite and siderite were present to varying degrees in all treatments. The size and morphology of goethite was similar for all treatments with an  $\text{MCD}_{111}$  of approximately 10 nm. Lepidocrocite ( $\gamma\text{-FeOOH}$ ) was detected by XRD only in the 0.5 and 1 mM lactate treatments with the greatest peak intensities observed at 0.5 mM. The form of lepidocrocite appeared to be highly crystalline (e.g.  $\text{MCD}_{104}$  of  $\sim 60$  nm). Hematite and magnetite were not detected.

In abiotic experiments with Fe(II), similar XRD patterns (not shown) were observed irrespective of Fe(II) concentrations and revealed that HFO was transformed to a mixture of crystalline Fe minerals including goethite, hematite (minor phase) and siderite. None of these phases were detected in Fe(II)-free controls treated in an identical manner confirming that Fe(II) alone can promote the transformation of HFO into the observed crystalline products.

$^{57}\text{Fe}$  Mössbauer spectroscopy was used to further characterize the resulting Fe phases from select treatments (Figure 7). Room temperature (RT) Mössbauer measurements confirmed the presence of microcrystalline goethite (collapsed sextet feature) in the 0.5, 5, and 20 mM lactate treatments (Figures 7a, b, and c). Our reported spectra are similar to those observed and interpreted by Mørup (1990). Mössbauer measurements at liquid  $\text{N}_2$  temperatures (77 K) were needed to resolve the spectra of the Fe(III) phases because of their small particle size (Figures 7d, e, and f). The 77 K Mössbauer spectra were sufficiently resolved to allow modeling of spectral areas. The HFO was transformed to a mixture of goethite (79%) and lepidoc-

rocite (21%) in the 0.5 mM lactate treatment (Figure 7d). As in Zachara et al. (2002) we equate spectral areas with mineral mass percent assuming a constant recoil factor for the different Fe(III) mineral phases. Ferrihydrite and lepidocrocite are not easily discriminated by Mössbauer analysis, but the XRD spectra of the mineral residue from the 0.5 mM experiment showed clear evidence for the presence of a significant mass percent of lepidocrocite (Figure 6a) and absence of ferrihydrite. The goethite content was at maximum in the 5 mM experiment (Figure 7e). Siderite, which was barely discernible at 5 mM lactate (Figure 7e), represented 12% of the Fe mass in the 20 mM sample.

## Discussion

The results from these investigations demonstrated that electron acceptor and donor concentrations can have profound effects on the rate and extent of HFO reduction and mineralogic transformations mediated by the DMRB *Shewanella putrefaciens* CN32. Also, it confirmed previous investigations (Zachara et al. 2002; Tronc et al. 1992) demonstrating that HFO is readily transformed to crystalline Fe minerals via abiotic reactions with Fe(II) under anoxic conditions suggesting that this may be an important mechanism in the biomineralization of HFO by DMRB. It should be pointed out that the observations reported in this manuscript may be specific for *S. putrefaciens* CN32 and that additional work is required to generalize these findings to other DMRB, including other *Shewanella* sp.

Under oxic conditions (e.g.  $p_e > 6$ ), HFO is thermodynamically unstable with respect to goethite and hematite (Figures 8a, b). However, the crystallization of HFO is kinetically slow at room temperature and typically occurs over periods of weeks to months at room temperature and in the absence of sorbates that can suppress crystallization (Fischer & Schwertmann 1975; Schwertmann & Murad 1983; Cornell & Giovanoli 1985). Low concentrations of sorbed  $\text{Fe}^{2+}$  have been shown to promote the recrystallization of HFO to goethite (Fischer, 1972). As  $p_e$  and the ratio of Fe(III)/(II) decrease, HFO becomes unstable with respect to magnetite and siderite (Figure 8c). Magnetite can form rapidly at circumneutral pH and higher within hours by topotactic/solid state conversion of HFO following  $\text{Fe(II)}_{\text{aq}}$  sorption (Cornell 1988; Mann et al. 1989; Tronc et al. 1992). As  $p_e$  and the ratio of Fe(III)/(II) decrease further in the presence of high bi-

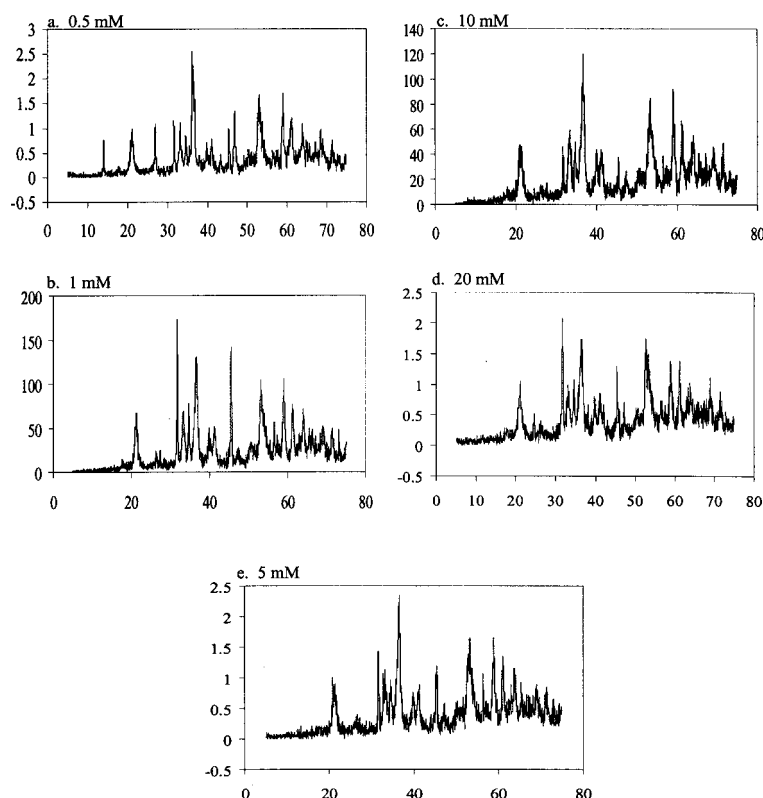


Figure 6. X-ray diffractograms of microbially reduced HFO under varying lactate concentrations: (a) 0.5 mM and (b) 20 mM.

carbonate concentrations and a headspace of  $N_2:CO_2$  (80:20), siderite solubility is exceeded.

The types and relative proportions of minerals formed in the biotic experiments varied with the different concentrations and ratios of electron donor to acceptor. The crystallization of HFO was competitive with its reduction by CN32 in these experiments. Crystallization of HFO to goethite and/or lepidocrocite resulted in a decreasing pool of HFO that was available for reduction by DMRB. Crystalline Fe(III) oxides are generally less bioreducible than HFO or ferrihydrite for thermodynamic and structural reasons (Lovley & Phillips 1986, 1987; Zachara et al. 1998) although a number of other factors including surface area and site concentration (Roden & Zachara 1996) may be equally or more important. Our results implied that the relative concentrations of electron donor and acceptor controlled the Fe(III) reduction/Fe(II) evolution rate. At high HFO concentration, some crystalline Fe(III) oxides were formed regardless of lactate concentration. Under these conditions, sorbed biogenic  $Fe^{2+}$  facilitated the formation of crystalline phases such as goethite, as observed in the abiotic experiment

with exogenous Fe(II). The rate of Fe(III) reduction decreased with increasing HFO:lactate ratios, resulting in a relatively greater proportion of crystalline Fe(III) phases of relatively low availability for DMRB. Although the respiration-driven rate of Fe(II) formation has been recognized as a significant factor governing the ferric and ferrous phases formed during bioreduction (Zachara et al. 2002), little is known about the quantitative ranges of biogenic Fe(II) flux and Fe(II) sorption density that lead to solid state recrystallization reactions (e.g. goethite, lepidocrocite, magnetite), or reductive dissolution/precipitation (e.g. siderite).

Another possible factor influencing the mineralization of HFO, in addition to the Fe(II) facilitated crystallization, is the interaction of HFO with the surfaces of CN32 cells. The cell envelopes of Gram-negative bacteria such as *Shewanella putrefaciens* typically carry a net negative charge and in general have a high capacity for binding cationic metals (Ferris 1989). CN32 was shown to have a relatively high capacity for Fe(II) sorption ( $4.19 \times 10^{-3}$  mol/ $10^{12}$  cells) and Fe precipitates of unknown valence and structure transiently formed on cell surfaces in sus-



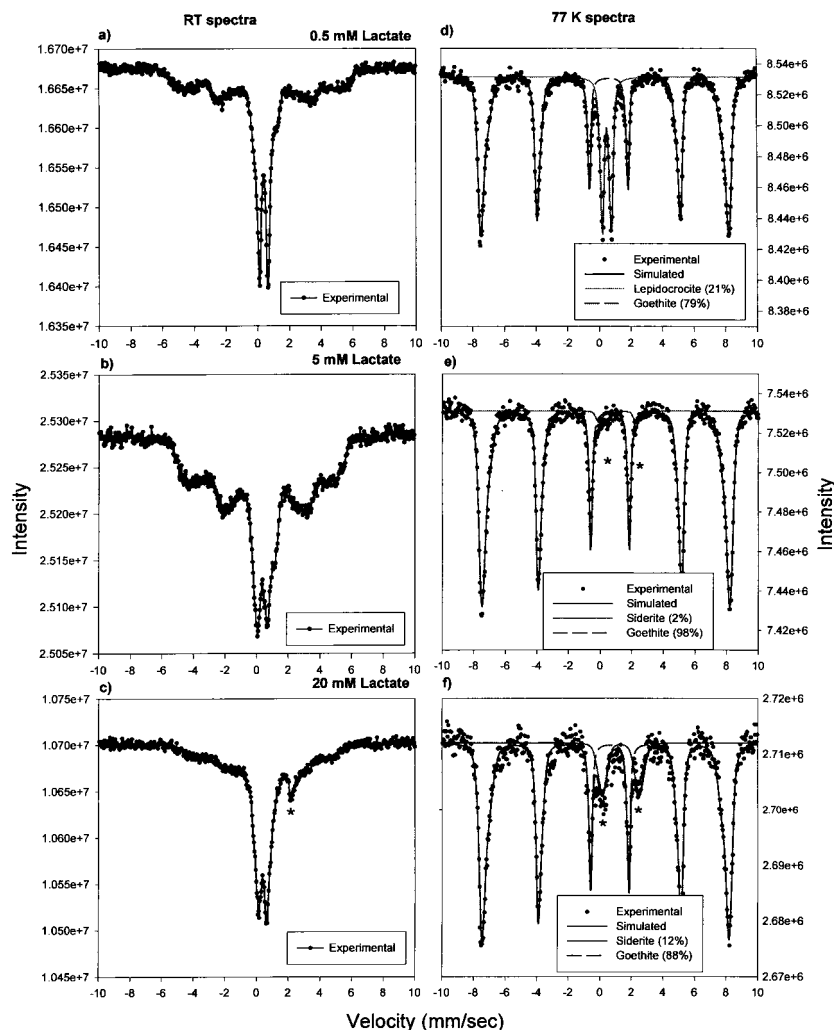


Figure 7. RT (a–c) and 77 K (d–f) Mössbauer spectra of Fe solids from the variable lactate treatment experiment: a & d – 0.5 mM lactate, b & e – 5 mM lactate and c & f – 20 mM lactate. For RT spectra data points were connected by line for clarity.

pensions that contained Fe(III)-citrate and that were spiked with Fe(II) (Liu et al. 2001). Little information is currently available regarding specific interactions between Fe(III) in general, and HFO specifically, and the surfaces of Gram-negative DMRB.

At low (5 and 10 mM) HFO concentrations without lactate limitation, >90% of the Fe(III) was bioreduced at a relatively rapid rate and no secondary minerals were observed (Table 1). In this case, the rate of HFO reduction was significantly greater than the rate of Fe(II)-facilitated crystallization, allowing for essentially complete reductive dissolution. Although not particularly strong complexants of Fe(II), the relatively high concentrations of lactate (30 mM initial), and acetate, a byproduct of anaerobic lactate oxida-

tion, would have contributed to the solubility of Fe(II) in these treatments, enhancing reductive dissolution. Previous research demonstrated that malate, as a result of complexation of Fe(II), enhanced the reduction of Fe(III) oxides by *Shewanella algae* strain BrY and promoted the solubilization of Fe(II) (Urrutia et al. 1998). At intermediate HFO:lactate ratios the rates of HFO reduction were competitive with the rates of crystallization allowing for both the formation of crystalline Fe(III) phases and the precipitation of siderite. As the bioreduction proceeds, the Fe(II) sorption capacity of HFO would be exceeded allowing the complexation of Fe(II) by carbonate, and an increase in aqueous concentration eventually exceeding siderite solubility. We have previously observed the formation

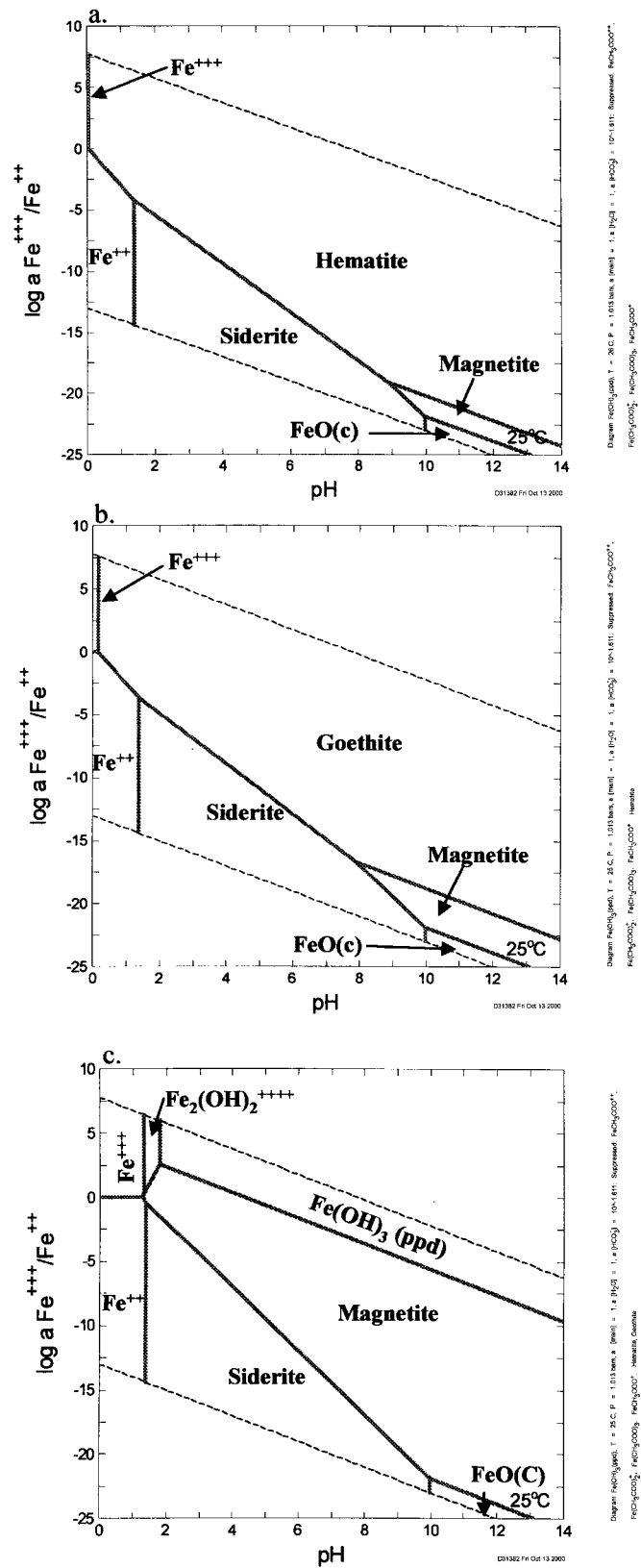


Figure 8. Thermodynamic stability of HFO at  $T = 25^\circ\text{C}$ ,  $P = 1.013 \text{ bars}$ ,  $\text{HCO}_3^- = 30 \text{ mM}$ . Plot showing stable minerals with respect to HFO: Hematite (a), Goethite (b), Magnetite and Siderite (a, b, c).

of highly crystalline siderite as a result of HFO bioreduction by CN32 in bicarbonate-buffered solutions (Fredrickson et al. 1998). High alkalinity and  $\text{Fe}_{(\text{aq})}^{2+}$  generated via microbial respiration promote siderite precipitation (Mortimer & Coleman 1997). Although the final pH values in the variable lactate (Table 1) and HFO (Table 2) experiments were circumneutral, microenvironments around actively respiring cells could create localized regions of elevated alkalinity and  $\text{Fe}_{(\text{aq})}^{2+}$  (Zachara et al. 2002). Although we observed siderite in bicarbonate-buffered HFO suspensions equilibrated with various concentrations of Fe(II) for 4 weeks, the abiotic precipitation of siderite can occur quite rapidly as illustrated by other studies where, at pH 7.2, siderite precipitation was 98% complete within 4 h when mmol/L solutions of Fe(II) and bicarbonate were mixed at room temperature (Thornber & Nickel 1976). In experiments with CN32 and HFO in MES [2-(N-morpholin)ethanesulfonic acid] or bicarbonate buffer, siderite was the only bioreduction product observed when the gas phase in the headspace of anaerobic CN32 cultures was 80:20,  $\text{N}_2$  to  $\text{CO}_2$  (Zachara et al. 2002). As the proportion of  $\text{N}_2$  to  $\text{CO}_2$  was increased to 90:10 and higher, additional phases including magnetite, goethite, and lepidocrocite were observed.

Various organic compounds can also retard or inhibit the crystallization of Fe(III) oxide from ferrihydrite in soils by binding to hydroxylated Fe(III) centers and functioning essentially as chemical defects (Schwertmann 1966). Long-term experiments carried out with HFO at 20 °C and at pH 6 in the presence of organic acids resulted in no detectable crystalline phases even after 12 months (Cornell & Schwertmann 1979). Cornell and Schwertmann (1979) reported that the influence of organic anions on the crystallization of ferrihydrite was dependent on adsorption to ferrihydrite that, in turn, was dependent upon pH and the functional groups involved. Lactate at pH 7 strongly adsorbs to HFO and, in the studies reported herein, approximately 50% of the lactate in all treatments is estimated to have sorbed to HFO. Although lactate is a relatively weak inhibitor of crystallization because it lacks a second COOH/OH pair required for bridging, at 10 mM ferrihydrite crystallization was retarded and at 1 M crystallization was completely inhibited (Cornell & Schwertmann 1979). Hence, the rate and extent of HFO bioreduction and the proportions of both crystalline Fe(III) oxides and of siderite formed in the experiments may have been influenced by lactate sur-

face complexation and its attendant effects on HFO crystallization.

An interesting result of the variable lactate and HFO bioreduction experiments and the abiotic Fe(II)-facilitated conversion of HFO experiment was the absence of detectable magnetite ( $\text{Fe}_3\text{O}_4$ ) in any of the treatments. Magnetite has been reported as a dominant phase resulting from the reduction of HFO by DMRB (Lovley 1991). Previous studies by our laboratory also observed the biogenic conversion of HFO to magnetite by CN32 but this phase was dominant only in PIPES-buffered medium where the  $\text{HCO}_3^-$  concentrations were  $< 3 \times 10^{-3}$  mol/L (Fredrickson et al. 1998). In bicarbonate buffered HFO suspensions in the previous studies, magnetite was not detected by XRD but was observed by transmission electron microscopy and energy dispersive X-ray elemental analysis as a minor phase in association with siderite. The absence of detectable magnetite in the abiotic experiments may have been due to the relatively low pH of the suspensions where sufficient Fe(II) was present and to the fact that XRD is relatively insensitive to phases present at  $< 5\%$  by mass. The relative stability of siderite and magnetite is quite sensitive to changes in pH over the range of values in our experiments with the neutral to moderately acid pH values favoring siderite and alkaline pH favoring magnetite (Bell et al. 1987; Zachara et al. 2002).

The results presented herein demonstrate that the relative concentrations of electron donor (lactate) and acceptor (HFO) had a significant impact on the rate and extent of HFO reduction and the type and proportions of Fe(III) and Fe(II) minerals formed. The conversion of HFO to more crystalline phases such as goethite and lepidocrocite was attributed to biogenic Fe(II) facilitated crystallization at relatively slow rates of bacterial respiration. The reasons for lepidocrocite formation in preference to goethite, and vice versa, were not resolved, but would make an interesting target for further study. These processes have important implications for Fe biogeochemistry as crystalline Fe(III) oxides are less available for reduction by DMRB relative to HFO (Lovley & Phillips 1987; Zachara et al. 1998). Unknown is the relative importance of these biologically mediated mineral transformations in natural environments. Nonetheless, they are anticipated to be important in sedimentary environments subject to seasonal changes in organic carbon input and oxidation state and in engineered systems where organic carbon is supplied to sediments to stimulate anaerobic microbial processes to facil-

itate the reductive immobilization of redox-sensitive metals. The results presented herein imply that Fe(II) oxides generation by DMRB may greatly hasten the transformation of poorly crystalline Fe(III) oxides to phases such as goethite and lepidocrocite. A microbiologic role in the *in situ* generation of these important and ubiquitous crystalline Fe(III) oxides is not well recognized.

## Acknowledgements

This research was funded by the U.S. Department of Energy (DOE), Office of Basic Energy Sciences, Engineering and Geosciences Division. Pacific Northwest National Laboratory is operated for the DOE by Battelle Memorial Institute under Contract DE-AC06-76RLO 1830. We also wish to thank David Kennedy and Chris Brown for XRD analyses, David Boone (Portland State University) for providing *S. putrefaciens* CN32 to us from the DOE Subsurface Microbial Culture Collection.

## References

- Arnold RG, DeChristina TJ & Hoffman MR (1988) Reductive dissolution of Fe(III) oxides by *Pseudomonas* sp. 200. *Biotechnol. Bioeng.* 32: 1081–1096
- Baedecker MJ, Cozzarelli IM, Evans JR & Hearn PP (1992) Authigenic mineral formations in aquifers rich in organic material. In: Kharaka YK & Maest AS (Eds) *Water-Rock Interaction: Proceedings of the 7th International Symposium* (pp. 257–261). Park City, Utah: A.A. Balkema Publishers
- Bell PE, Mills AL & Herman JS (1987) Biogeochemical conditions favoring magnetite formation during anaerobic iron reduction. *Appl. Environ. Microbiol.* 53: 2610–2616
- Cornell RM (1988) The influence of some divalent cations on the transformation of ferrihydrite into more crystalline products. *Clays Clay Miner.* 23: 329–332
- Cornell RM & Schwertmann U (1979) The influence of organic anions on the crystallization of ferrihydrite. *Clays Clay Miner.* 27: 402–410
- Cornell RM & Giovanoli R (1985) Effect of solution conditions on the proportion and morphology of goethite formed from ferrihydrite. *Clays Clay Miner.* 33: 424–432
- Dong H, Fredrickson JK, Kennedy DW, Zachara JM, Kukkadapu RK & Onstott TC (2000) Mineral transformation associated with the microbial reduction of magnetite. *Chem. Geology* 169: 299–318
- Ferris FG (1989) Metallic ion interactions with the outer membrane of Gram-negative bacteria. In: Beveridge TJ & Doyle RJ (Eds) *Metal ions and bacteria* (pp. 295–323). New York: John Wiley & Sons
- Fischer WR (1972) Die wirkung von zweitwertigem eisen auf losung umwandlung von eisen(III)-hydroxiden. In: Schlichting E & Schwertmann U (Eds) *Pseudogley and Gley Trans Comm V and VI Int Soil Sci Soc.* (pp. 37–44). VCH, Weinheim
- Fischer WR & Schwertmann U (1975) The formation of hematite from amorphous iron(III)-hydroxide. *Clays Clay Miner.* 23: 33–37
- Fredrickson JK, Zachara JM, Kukkadapu RK, Gorby YA, Smith SC & Brown CF (2001) Biotransformation of Ni-substituted hydrous ferric oxide by an Fe(III)-reducing bacterium. *Environ. Sci. Technol.* 35: 703–712
- Fredrickson JK, Zachara JM, Kennedy DW, Dong H, Onstott TC, Hinman NW & Li SW (1998) Biogenic iron mineralization accompanying the dissimilatory reduction of hydrous ferric oxide by a groundwater bacterium. *Geochim. Cosmochim. Acta* 62: 3239–3257
- Heron G & Christensen TH (1995) Impact of sediment-bound iron on redox buffering in a landfill leachate polluted aquifer (Vejen, Denmark). *Environ. Sci. Technol.* 29: 187–192
- Kostka JE & Nealson KH (1995) Dissolution and reduction of magnetite by bacteria. *Environ. Sci. Technol.* 29: 2535–2540
- Kukkadapu RK, Zachara JM, Smith SC, Fredrickson JK & Liu C (2001) Dissimilatory bacterial reduction of Al-substituted goethite in subsurface sediments. *Geochim. Cosmochim. Acta* 65: 913–2924
- Liu CG, Zachara JM, Gorby YA, Szecsody JE & Brown CF (2001) Microbial reduction of Fe(III) and sorption/precipitation of Fe(II) on *Shewanella putrefaciens* strain CN32. *Environ. Sci. Technol.* 35: 1385–1393
- Lovley D (1995) Bioremediation of organic and metal contaminants with dissimilatory metal reduction. *J. Indust. Microbiol.* 14: 85–93
- Lovley DR (1991) Magnetite formation during microbial dissimilatory iron reduction. In: Frankel RB & Blakemore RP (Eds) *Iron biominerals* (pp. 151–166). Plenum Press, New York
- Lovley DR (1993) Dissimilatory metal reduction. *Annu. Rev. Microbiol.* 47: 263–290
- Lovley DR & Phillips EJP (1986) Availability of ferric iron for microbial reduction in bottom sediments of the freshwater tidal Potomac River. *Appl. Environ. Microbiol.* 52: 751–757
- Lovley DR & Phillips EJP (1988) Novel mode of microbial energy metabolism: organic carbon oxidation coupled to dissimilatory reduction of iron or manganese. *Appl. Environ. Microbiol.* 54: 1472–1480
- Lovley DR & Lloyd JR (2000) Microbes with a mettle for bioremediation. *Nature Biotech.* 18: 600–601
- Lovley DR, Phillips EJP & Lonergan DJ (1989a) Hydrogen and formate oxidation coupled to dissimilatory reduction of iron or manganese by *Alteromonas putrefaciens*. *Appl. Environ. Microbiol.* 55: 700–706
- Lovley DR, Baedecker MJ, Lonergan DJ, Cozzarelli IM, Phillips EJP & Siegal DI (1989b) Oxidation of aromatic contaminants coupled to microbial iron reduction. *Nature* 339: 297–299
- Lovley RR & Phillips EJP (1987) Rapid assay for microbially reducible ferric iron in aquatic sediments. *Appl. Environ. Microbiol.* 53: 1536–1540
- Mann S, Sparks NHC, Couling SB, Larcombe MC & Frankel RB (1989) Crystallochemical characterization of magnetic spinels prepared from aqueous solution. *J. Chem. Soc. Faraday Trans.* 85: 3033–3044
- Mortimer RJG & Coleman ML (1997) Microbial influence on the isotopic composition of diagenetic siderite. *Geochim. Cosmochim. Acta* 61: 1705–1711
- Morup S (1990) Mössbauer effect on small particles. *Hyperfine Interactions* 60: 959–974
- Murad E & Schwertmann U (1984) The influence of crystallinity on the Mössbauer spectrum of lepidocrocite. *Mineralogical Magazine* 48: 507–511

- Nealson K & Saffarini D (1994) Iron and manganese in anaerobic respiration: environmental significance, physiology, and regulation. *Annu. Rev. Microbiol.* 48: 311–343
- Rancourt DG & Ping JY (1991) Voight-based methods for arbitrary-shape static hyperfine parameter distributions in Mössbauer spectroscopy. *Nucl. Instrum. Meth. Phys. Res. B* 58: 85–97
- Roden EE & Zachara JM (1996) Microbial reduction of crystalline Fe(III) oxides: influence of oxide surface area and potential for cell growth. *Environ. Sci. Technol.* 30: 1618–1628
- Roden EE & Urrutia MM (1999) Ferrous iron removal promotes microbial reduction of crystalline iron(III) oxides. *Environ. Sci. Technol.* 33: 1847–1853
- Roden EE, Urrutia MM & Mann CJ (2000) Bacterial reductive dissolution of crystalline Fe(III) oxide in continuous-flow column reactors. *Appl. Environ. Microbiol.* 66: 1062–1065
- Roden ER & Lovley DR (1993) Dissimilatory Fe(III) reduction by the marine microorganism *Desulfuromonas acetooxidans*. *Appl. Environ. Microbiol.* 59: 734–742
- Schwertmann U (1966) Inhibitory effect of soil organic matter on the crystallization of amorphous ferric hydroxide. *Nature* 212: 645–646
- Schwertmann U & Murad E (1983) Effect of pH on the formation of goethite and hematite from ferrihydrite. *Clays Clay Miner.* 31: 277–284
- Sidhu PS, Gilkes RJ, Cornell RM, Posner AM & Quirk JP (1981) Dissolution of iron oxides and oxyhydroxides in hydrochloric and perchloric acids. *Clays Clay Miner.* 29: 269–276
- Thorner MR & Nickel EH (1976) Supergene alteration of sulphide. III. The composition of carbonates. *Chem. Geology* 17: 45–72
- Tronc E, Belleville P, Jolivet JP & Livage J (1992) Transformation of ferric hydroxide into spinel by Fe(II) adsorption. *Langmuir* 8: 313–319
- Urrutia MM, Roden EE & Zachara JM (1999) Influence of aqueous and solid-phase Fe(II) complexants on microbial reduction of crystalline iron(III) oxides. *Environ. Sci. Technol.* 33: 4022–4028
- Urrutia MM, Roden EE, Fredrickson JK & Zachara JM (1998) Microbial and surface chemistry controls on reduction of synthetic Fe(III) oxide minerals by the dissimilatory iron-reducing bacterium *Shewanella alga*. *Geomicrobiol. J.* 15: 269–291
- Zachara JM, Kukkadapu RK, Fredrickson JK, Gorby YA & Smith SC (2002) Biomineralization of poorly crystalline Fe(III) oxides by dissimilatory metal reducing bacteria (DMRB). *Geomicrobiol. J.* 19: 179–207
- Zachara JM, Fredrickson JK, Li SW, Kennedy DW, Smith SC & Gassman PL (1998) Bacterial reduction of crystalline Fe<sup>3+</sup> oxides in single phase suspensions and subsurface materials. *Am. Miner.* 83: 1426–1443